Structural Transitions Accompanying the Activation of Peptide Binding to the Endoplasmic Reticulum Hsp90 Chaperone GRP94†

Pamela A. Wearsch, Laura Voglino, and Christopher V. Nicchitta*

Department of Cell Biology, Duke University Medical Center, Durham, North Carolina 27710

Received January 13, 1998; Revised Manuscript Received February 27, 1998

ABSTRACT: GRP94, the endoplasmic reticulum Hsp90 paralog, binds a diverse array of peptides, a subset of which are suitable for assembly onto nascent MHC class I molecules. At present, the mechanism, site, and regulation of peptide binding to GRP94 are unknown. Using VSV8, the immunodominant peptide epitope of the vesicular stomatitis virus, and native, purified GRP94, we have investigated GRP94−peptide complex formation. The formation of stable GRP94−VSV8 complexes was slow; competition studies demonstrated that peptide binding to GRP94 was specific. VSV8 binding to GRP94 was stimulated 2-fold or 4-fold, respectively, following chemical denaturation/renaturation or transient heat shock. The activation of GRP94−peptide binding occurred coincident with a stable, tertiary conformational change, as identified by tryptophan fluorescence and proteolysis studies. Analysis of GRP94 secondary structure by circular dichroism spectroscopy indicated an identical α-helical content for the native, chemically denatured/renatured, and heat-shocked forms of GRP94. Through use of the environment-sensitive fluorophores acrylodan and Nile Red, it was observed that the activation of peptide binding was accompanied by enhanced peptide and solvent accessibility to a hydrophobic binding site(s). Peptide binding to native or activated GRP94 was identical in the presence or absence of ATP or ADP. These results are discussed with respect to a model in which peptide binding to GRP94 occurs within a hydrophobic binding pocket whose accessibility is conformationally regulated in an adenine nucleotide-independent manner.

GRP94 (gp96), the endoplasmic reticulum (ER) paralog of Hsp90,[1] participates in the protein folding and assembly reactions that accompany protein translocation in the ER. A chaperone function for GRP94 has been inferred from observations that GRP94 expression is up-regulated by conditions that stimulate the accumulation of unfolded proteins in the ER (*1*−*5*). In addition, GRP94 has been identified in association with a number of structurally immature protein folding intermediates (*6*−*9*). Studies on immunoglobulin light chain assembly indicate that GRP94 may function at a relatively late stage of protein folding. When the kinetics of BiP and GRP94 interaction with folding light chains were investigated, GRP94 was found to associate with lights chains after BiP (*8*). At present, the sequence and/or structural motifs recognized by GRP94 are unknown.

In addition to its role in protein folding and assembly, recent experimental evidence indicates that GRP94 functions as a peptide binding protein and, in this context, contributes to the peptide trafficking pathways that provide peptide ligands to nascent MHC class I molecules. That GRP94 functions as a peptide binding protein was first noted in tumor immunology studies of MethA chemically induced sarcomas. In these studies, mice vaccinated with murine MethA sarcoma-derived GRP94 displayed protective immunity to challenges with cells derived from the parent tumor (*10*, *11*). The observations that MethA sarcoma-derived GRP94 was identical in sequence to tissue-derived GRP94 (*12*), and that tissue-derived GRP94 did not confer protective immunity, indicated that immunity was conferred not by GRP94 per se but rather through a pool of stably bound peptides. This observation has been confirmed and extended in more recent immunological studies demonstrating that GRP94 from a wide array of cells copurifies with host cell-specific peptides (*11*, *13*−*16*).

GRP94 can elicit an MHC class I response to peptide antigens originating in the cells from which it was derived (*13*, *14*, *17*). As it is well established that peptide antigens destined for assembly onto MHC class I molecules are predominantly generated in the cytosol, and subsequently transported into the ER via the TAP transporter (*18*), these observations suggest that the GRP94-derived peptides are transported from the extracellular space to the ER, presumably while in complex with GRP94, at which point the peptides become available for selection as class I ligands. At present, the trafficking pathway(s) that mediate(s) transport of GRP94−peptide complexes from the extracellular space to the cytosol and/or the ER is (are) unknown (*19*).

For some MHC class I alleles, physical interaction of the class I heavy chain/β_2-microglobulin complexes with TAP appears to be required for peptide loading, suggesting that TAP-dependent peptide transport is directly coupled to

† Support for these studies was provided by a grant from the NIH (DK53058)(C.V.N.).

* To whom correspondence should be addressed. Phone: (919) 684-8948. Fax: (919) 684-5481. E-mail: C.Nicchitta@cellbio.duke.edu.

[1] Abbreviations: AR, acrylodan; CD, circular dicroism; GdmCl, guanidinium chloride; Hsp, heat shock protein; MHC, major histocompatibility complex; R_s, Stokes radius; TAP, transporter associated with antigen processing; VSV, vesicular stomatitis virus.

S0006-2960(98)00100-7 CCC: $15.00
Published on Web 04/03/1998

peptide/MHC class I assembly (*20*−*23*). In this scenario, GRP94-derived peptides destined for assembly onto class I molecules would necessarily traffic to the ER via the TAP-dependent pathway. However, it has also been reported that several class I alleles acquire peptides in the absence of stable interactions with TAP, or in the absence of TAP itself (*24*−*26*). Should peptide loading onto class I molecules not be directly coupled to TAP-mediated transport, a scenario in which transfer of GRP94-derived peptides to class I molecules, by an as of yet unknown mechanism, becomes possible. In this regard, it is important to note that GRP94 binds peptides whose appearance in the ER is either TAP-dependent or TAP-independent (*27*−*31*). Although the relative contribution and physiological regulation of GRP94-mediated peptide transfer to class I molecules remain to be established, it appears likely that peptide binding to GRP94 and other ER chaperones functions to maintain a repertoire of peptides within the ER, a subset of which can be selected for assembly onto class I molecules.

Although little is known regarding the regulation of peptide binding to GRP94, recent structural studies of the cytosolic Hsp90's suggest important regulatory functions for a highly conserved structural domain located in the N-terminal region of the protein (*32*−*34*). The functional significance of this domain is indicated by both mutational analysis (*35*−*38*) and crystal structure studies, which identify a binding pocket serving as the site of interaction for the antitumor drug geldanamycin (*34*) and ATP/ADP (*33*). Stebbins et al. (*34*) have identified two, atomically resolved alternate conformations of this domain, which they refer to as the "open" and "closed" conformations. It is only in the "open" conformation that the binding pocket is solvent, and thus geldanamycin, accessible, leading the authors to suggest that conformational conversions between the two forms are likely to serve a role in the regulation of Hsp90 function. Crystal structure studies of the equivalent domain isolated from yeast Hsp90 indicate that the N-terminal domain functions as a dimer and the highly conserved pocket serves as an ATP/ADP binding site (*33*). From these structural data, it has been proposed that cycles of ATP binding and hydrolysis function to recruit accessory proteins, which themselves modulate structural interactions between the two Hsp90 subunits (*33*).

In this communication, we present data demonstrating that peptide binding to GRP94 is markedly activated following transient heat shock or chemical denaturation/renaturation. The activation of peptide binding is accompanied by a conformational change that substantially increases solvent and peptide accessibility to a hydrophobic domain. Peptide binding to both native and activated GRP94 is specific and, under the assay conditions defined in this study, independent of ATP or ADP. The implications of these findings on the mechanism and regulation of GRP94 chaperone activity are discussed.

EXPERIMENTAL PROCEDURES

Purification of GRP94 and BiP. GRP94 and BiP were purified from porcine pancreas rough microsomes as described previously (*39*), with the following modifications. Rough microsomes were washed in 0.25 M sucrose, 20 mM KOAc, 25 mM K-Hepes, pH 7.2, 5 mM $Mg(OAc)_2$, and membrane permeabilization was performed with 4 mM CHAPS. Protein concentrations were determined using the BCA protein assay (Pierce, Rockford, IL) for BiP or the absorbance at 280 nm for GRP94 (1.18 mg/mL = 1 A_{280}). The molar concentrations of GRP94 and BiP were determined using the subunit molecular masses of 92 500 and 72 000 Da, respectively.

Pretreatment of GRP94 by Heat Shock and Chemical Denaturation. For the temperature activation of peptide binding, GRP94 at 0.5 mg/mL in buffer A [110 mM KOAc, 20 mM NaCl, 25 mM K-Hepes, pH 7.2, 2 mM $Mg(OAc)_2$, 0.1 mM $CaCl_2$] was heated at 50 °C for 15 min and cooled for 10 min at RT. For activation by chemical denaturation/renaturation, GRP94 at a concentration of 0.75 mg/mL was incubated in 3 M GdmCl for 12 h at 4 °C. GRP94 was then dialyzed in 8000 MWCO dialysis tubing (Spectrapor, Houston, TX) against 1 L of buffer A for 6 h, with buffer exchange at 3 h.

[^{125}I]C-VSV8 Binding Assay. The peptides C-VSV8 (sequence CRGYVYQGL) and C-H5 (sequence CLGYEDAWS) were synthesized by Research Genetics Inc. (Huntsville, AL) using standard F-moc chemistry and desalted on a Sephadex G-10 column equilibrated in 30% acetonitrile. C-VSV8 was iodinated using the Iodobeads procedure (Pierce, Rockford, IL). Typically, 200 μg of C-VSV8 was incubated with 0.5 mCi of Na^{125}I in 250 μL of 25 mM Tris-HCl, pH 7.0, for 15 min at RT. The iodinating reagent was removed from the reaction mixture, and the free radioisotope was removed by three 1 h incubations with 15 mg of DOWEX 1×8-50 beads (Sigma, St. Louis, MO). [^{125}I]C-VSV8 specific activity varied between 0.25 and 0.35 μCi/μg.

To analyze peptide binding to GRP94, 1 μM each of native, temperature-treated, and GdmCl-treated GRP94 was incubated with 10 μM [^{125}I]C-VSV8 in 100 μL of buffer A for 90 min at 37 °C. Where indicated, a 50-fold molar excess of unlabeled C-VSV8 or C-H5 was included. Bound versus free peptide were resolved by gel filtration chromatography on a 5 mL S-200 column equilibrated in buffer A. The quantity of bound peptide in the GRP94-containing fractions was determined by γ-counting of the eluted fractions. Reactions were performed in triplicate, and background values (peptide minus GRP94) were subtracted.

Preparation of Peptide−*Acrylodan Conjugate*. The acrylodan−peptide conjugate (VSV8−AR) was prepared in a 1 mL reaction containing 500 μM acrylodan (Molecular Probes, Eugene, OR), 250 μM C-VSV8, 10 mM K-Hepes, pH 7.2, and 30% acetonitrile. Incubations were performed for 2 h on ice and quenched by the addition of 5 mM β-mercaptoethanol. VSV8−AR was desalted by chromatography on a 15 mL Sephadex G-10 column equilibrated in 30% acetonitrile. The VSV8−AR-containing fractions were pooled and concentrated to 1 mL by vacuum centrifugation. Final conjugate concentrations were determined by quantitative amino acid analysis (Duke University Medical Center, Protein Sequencing Facility) and spectrophotometrically using an extinction coefficient of 12 900 M^{-1} cm^{-1} at 360 nm (*40*). The chemical identity of VSV8−AR was confirmed by plasma desorption mass spectrometry (Duke University Medical Center, Protein Sequencing Facility) and C_{18} analytical HPLC with fluorescence detection at 510 nm. The acrylodan:peptide ratio was 1:1.

Fluorescence Measurements. Fluorescence measurements were conducted in a Fluoromax spectrofluorometer (Spex Industries, Inc., Edison, NJ) in 250 μL quartz cuvettes using a custom-thermostated cuvette chamber at 25 °C. Slit widths were set at 1 nm for both excitation and emission. Emission spectra were corrected by background subtraction of buffer samples.

To analyze for peptide−acrylodan binding, native, GdmCl-treated, and temperature-treated GRP94 (1 μM final concentration) were incubated with 20 nM VSV8−AR for 30 min at 37 °C in 250 μL of buffer A. Binding reactions were performed in siliconized microtubes (PGC Scientifics, Frederick, MD) to reduce nonspecific adsorption of the VSV8−AR conjugate. Where indicated, 100 μM ATP or ADP (Boehringer Mannheim, Indianapolis, IN) was included in the binding reaction. Samples were transferred to quartz cuvettes, and emission scans were collected with excitation at 360 nm. For investigations into the temperature dependence of peptide binding, native GRP94 (1 μM) was incubated with 50 nM VSV8−AR for 30 min in buffer A at temperatures ranging from 25 to 65 °C. The relative binding was determined by the fluorescence intensity at 460 nm, the emission maximum for GRP94-bound VSV8−AR.

Intrinsic GRP94 tryptophan fluorescence was determined at an excitation wavelength of 295 nm. To monitor the unfolding transitions of GRP94 in GdmCl, native GRP94 at 75 μg/mL in buffer A was incubated with increasing concentrations of GdmCl for 1 h at RT. A denaturation curve was generated by measuring the fluorescence intensity at 335 nm, the tryptophan emission wavelength maximum for native GRP94. To compare the intrinsic tryptophan fluorescence between the native, activated, and denatured GRP94, 75 μg/mL of each pool in 250 μL of buffer A was analyzed at RT. The denatured GRP94 sample for this experiment represented GRP94 analyzed in the presence of 3 M GdmCl.

Nile Red (Molecular Probes) binding studies were performed at a Nile Red concentration of 1 μM with 0.5 μM native, GdmCl-treated, and temperature-treated GRP94 for 15 min at 37 °C. Emission spectra (570−700 nm) were collected at an excitation wavelength of 550 nm. For the analysis of the temperature dependence of Nile Red binding, 1 μM Nile Red was added to 0.5 μM native GRP94 in 250 μL of buffer A, and incubations were performed for 15 min at temperatures ranging from 25 to 65 °C. The change in fluorescence intensity at 615 nm (the emission maximum of GRP94-bound Nile Red) was used as the measure of binding.

Circular Dichroism Measurements. Far-UV CD spectrometry was used to analyze GRP94 secondary structure following the GdmCl and temperature treatments. All measurements were obtained with the AVIV Associates (Lakewood, NJ) circular dichroism spectrometer, Model 62DS. Samples were analyzed in 0.1 cm path length quartz cuvettes at RT. For GdmCl denaturation studies, 1 μM GRP94 was incubated in 5 mM K-Hepes, pH 7.2, with 0−5 M GdmCl for 20 h at RT prior to analysis. Samples (1 mL) were then renatured by dialysis against 1 L of 5 mM K-Hepes, pH 7.2, for 4 h at 4 °C, with buffer exchange at 2 h. The α-helical content of native GRP94 was calculated from the molar ellipticity at 222 nm, as described in Chen et al. (*41*). For the comparison of native and temperature-treated GRP94, samples were dialyzed into a buffer consisting of 50 mM KOAc, 10 mM K-Hepes, pH 7.2, and the far-UV CD spectrum of a 1.25 μM GRP94 solution was recorded from 260 to 190 nm. The mean residue ellipticity was calculated from the data using a mean residue molecular weight of 118.

Analytical Gel Filtration Chromatography. The quaternary structure of GRP94 was analyzed by analytical gel filtration chromatography on a TSK-GEL G3000 SW column (Tosohaus, Montgomeryville, PA) equilibrated in buffer A. Detection was by the absorbance at 280 nm. The column was calibrated with proteins of known Stokes radii (R_s), as previously described (*42*). To determine the concentration dependence of temperature-dependent oligomer formation, GRP94 (12.5 μg per sample) was treated at 50 °C for 15 min, at concentrations ranging from 0.5 to 15 μM, in buffer A. After cooling for 10 min at RT, samples were brought up to a final volume of 125 μL and analyzed. The molecular weight and oligomerization state of the temperature-treated and GdmCl-treated GRP94 were calculated as previously described (*42*) using the average R_s, determined by gel filtration, and the sedimentation coefficient, determined by velocity sedimentation (data not shown).

Proteolytic Digestion of GRP94. Native, temperature-treated, and GdmCl-treated GRP94, at a concentration of 0.15 mg/mL, were digested by the addition of chymotrypsin (0.25−10% w/w) or elastase (0.5−10% w/w) for 20 min at 30 °C in 25 μL of buffer A. Reactions were terminated by the addition of 10% TCA, and samples were processed for SDS−PAGE as described (*42*).

ATP Binding Assay. ATP binding assays were performed as previously described (*39*). In brief, 0.35 μM each of GRP94, BiP, and BSA were incubated with 100 μM [α-^{32}P]-ATP for 1 h at 30 °C in 100 μL of 110 mM KOAc, 20 mM NaCl, 25 mM K-Hepes, pH 7.2, 5 mM $Mg(OAc)_2$, 0.1 mM $CaCl_2$. The reactions were performed in the absence or presence of a 50-fold molar excess of unlabeled ATP or ADP. The bound nucleotide was separated from free by vacuum filtration on BA85 filters (Schleicher & Schuell, Keene, NH) using a manifold vacuum filtration device (Pharmacia, Piscataway, NJ). The specific activity of the [α-^{32}P]ATP was 80 μCi/μmol. Binding reactions were performed in triplicate, and [α-^{32}P]ATP bound in the absence of protein was subtracted as background from all points.

RESULTS

Activation of GRP94 Peptide Binding Activity. VSV8, the immunodominant peptide epitope of the vesicular stomatitis virus (VSV), has been identified as a native GRP94 ligand in VSV-infected cells, and has been demonstrated to bind to GRP94 in vitro (*14*, *15*, *39*, *43*). On the basis of the unusual kinetic stability of GRP94−peptide complexes, and an unexpectedly high apparent dissociation constant for VSV8 binding, it was proposed that there exists a kinetic barrier to VSV8 binding (*39*). Studies were thus initiated to determine if peptide binding to GRP94 was rate-limiting with respect to the dissociation of bound peptides, GRP94 conformational state, or both. Two experimental conditions were identified that stimulated GRP94 peptide binding activity: a single cycle of denaturation/renaturation in guanidinium chloride (GdmCl-treated) or transient heat shock (temperature-treated). Data depicting these observations are detailed in Figure 1. In this experiment, 1 μM GRP94 was

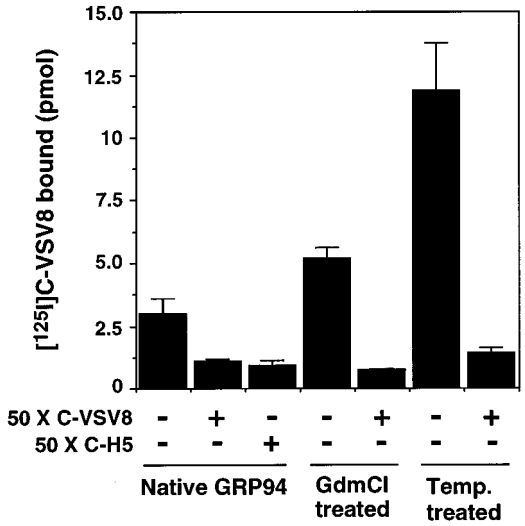

FIGURE 1: Binding of [^{125}I]C-VSV8 to native and activated GRP94 pools. Native, GdmCl-treated, and temperature-treated forms of GRP94, at a concentration of 1 μM, were incubated with 10 μM [^{125}I]C-VSV8 for 90 min at 37 °C. Where indicated, a 50-fold molar excess (0.5 mM) of unlabeled C-VSV8 or C-H5 was included in the binding reaction. The bound versus free peptide was resolved by Sephacryl S-200 gel filtration chromatography. Reactions were performed in triplicate.

incubated with 10 μM [^{125}I]C-VSV8 for 90 min at 37 °C, and the bound vs free peptide was resolved by gel filtration chromatography. C-VSV8 represents the VSV8 sequence synthesized with an additional cysteine residue at the N-terminus. Binding of VSV8 to native GRP94 was slow (data not shown), and was stimulated approximately 2-fold and 4-fold following chemical denaturation/renaturation or transient heat shock, respectively (Figure 1). Under all conditions assayed, [^{125}I]C-VSV8 binding was markedly inhibited in the presence of excess, unlabeled peptide. Furthermore, [^{125}I]C-VSV8 binding was blocked by the addition of a 50-fold excess of the peptide C-H5 (Figure 1), consistent with observations that GRP94 binds a diverse array of peptides (*28*, *29*, *31*).

Peptide Binding to a Hydrophobic Binding Pocket. To characterize the physical characteristics of the GRP94 peptide binding site, VSV8 was conjugated to an environment-sensitive fluorophore, acrylodan. Acrylodan−peptide conjugates have proven to be valuable probes for the study of peptide−chaperone interactions and can be used to resolve the kinetics of such interactions and to gain insight into the relative polarity of the peptide binding site (*40*, *44*, *45*).

Acrylodan is a dimethylaminonaphthalene derivative whose spectral properties vary with solvent polarity (*40*). This behavior is shown in Figure 2A, which depicts the emission spectra of the β-mercaptoethanol adduct of acrylodan (βME−acrylodan) in solvents of decreasing polarity. As illustrated, βME−acrylodan displayed a fluorescence emission maximum at 525 nm in water, whereas in solvents of decreasing polarity the emission maxima undergo a characteristic blue-shift and the fluorophore displays an increased quantum yield (*40*).

It is by the same principle shown in Figure 2A that the physical characteristics of the GRP94 peptide binding site can be assessed. Acrylodan was conjugated to the cysteine residue of C-VSV8, and the purity and identity of the conjugate (referred to as VSV8−AR) were confirmed by

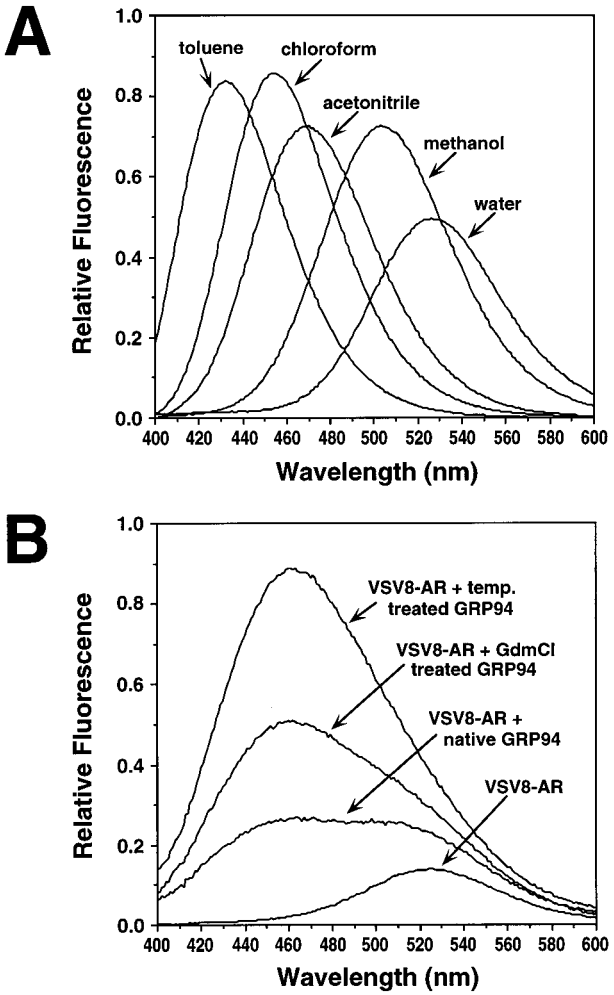

FIGURE 2: Spectral properties of acrylodan and binding of peptide−AR conjugates to GRP94. (A) Spectral properties of acrylodan. The emission spectra of βME−acrylodan were determined in the following solvents at the following concentrations: water, 500 nM; methanol, 100 nM; acetonitrile, 40 nM; chloroform, 45 nM; toluene, 50 nM. (B) Binding of VSV8−AR to native and activated GRP94 species. GRP94 (1 μM) was incubated with 20 nM VSV8−AR for 30 min at 37 °C. The emission spectra were recorded from 400 to 600 nm with an excitation wavelength of 360 nm. Excitation and emission slit widths were 1 nm. The VSV8−AR spectrum was determined at a concentration of 20 nM.

mass spectrometry and quantitative amino acid analysis. Similar to βME−acrylodan, free VSV8−AR displayed an emission maximum of 525 nm in aqueous buffers (Figure 2B). To determine the spectral properties of GRP94-bound VSV8−AR, 1 μM each of native and activated GRP94 was incubated with 20 nM VSV8−AR for 30 min at 37 °C, and the emission spectra were determined (Figure 2B). The emission spectra of VSV8−AR incubated in the presence of GRP94 were blue-shifted with an emission maxima of 465 nm and accompanied by a substantial increase in fluorescence yield (Figure 2B). These spectral changes indicated that bound peptide resides in a substantially apolar environment. Consistent with the results from the [^{125}I]C-VSV8 binding assay (Figure 1), native GRP94 displayed the lowest VSV8−AR binding activity, whereas GdmCl-treated and temperature-treated GRP94 displayed 2-fold and 4-fold increases in binding, respectively (Figure 2B). It is noteworthy that the emission maximum of bound VSV8−AR was identical for native, GdmCl-treated, and temperature-

treated GRP94, indicating that the physical environment of the GRP94-bound VSV8−AR ligand was similar, if not identical, for all forms of GRP94.

Exposure of a Hydrophobic Pocket Correlates with the Activation of GRP94 Peptide Binding Activity. In context of the data describing the existence of a relatively hydrophobic peptide binding site(s), as indicated by the spectral characteristics of GRP94-bound peptide−acrylodan conjugates, additional experiments were performed to determine if the activation of peptide binding was associated with changes in solvent accessibility to the hydrophobic binding site(s). These studies were performed with Nile Red, an environment-sensitive probe for hydrophobic protein surfaces (*46*). Nile Red displays an emission wavelength maximum at 645 nm and, similar to acrylodan, exhibits a blue-shift and increased fluorescence yield in apolar environments (*46*). Native and temperature-treated GRP94 at a concentration of 0.5 μM were incubated with Nile Red (1 μM) for 15 min at 37 °C, and the emission spectra were determined (Figure 3A). No shift in Nile Red emission maximum was observed in the presence of native GRP94; however, a shoulder was apparent in the emission spectrum, with a maximum at 615 nm (Figure 3A). Control experiments indicated that the observed higher relative fluorescence was due to both a decrease in nonspecific adsorption of the probe to the cuvette in the presence of added protein and the enhanced fluorescence yield accompanying the relatively low-level binding of the probe to the native protein (46; data not shown). In the presence of temperature-treated GRP94, a blue-shift in the Nile Red emission maximum to 615 nm and a corresponding increase in fluorescence intensity were observed (Figure 3A). A similar shift in the Nile Red emission maximum for GdmCl-treated GRP94 was also observed (data not shown). It can be concluded from these spectral differences that the Nile Red binding site(s) on the activated GRP94 molecules possess(es) a significant, and similar, hydrophobic character. It is also apparent that the Nile Red binding site(s) on native GRP94 is (are) relatively inaccessible.

To further explore the relationship between peptide binding and the exposure of the hydrophobic pocket, VSV8−AR binding and Nile Red binding to native GRP94 were compared over a temperature range from 25 to 65 °C (Figure 3B,C). It is clear from these experiments that the enhanced binding of Nile Red that is observed upon incubation at increasing temperatures is closely paralleled by an increase in VSV8−AR binding. These data suggest that the temperature-sensitive appearance of enhanced Nile Red binding may be related to the temperature-dependent activation of peptide binding. One possibility which is consistent with the data is that Nile Red binds to the peptide binding site, which is relatively inaccessible in the native state, yet is exposed as a result of the conformational changes that accompany GdmCl and temperature treatments.

GdmCl and Temperature Treatments Do Not Alter GRP94 Secondary Structure. To investigate the structural basis for the activation of GRP94 peptide binding activity by heat shock or chemical denaturation/renaturation, far-UV circular dichroism (CD) studies were performed. First, the GdmCl denaturation/renaturation profile of GRP94 was performed. Analysis of the CD spectra of native GRP94 indicated an α-helical content of 41%; a nearly complete loss of the

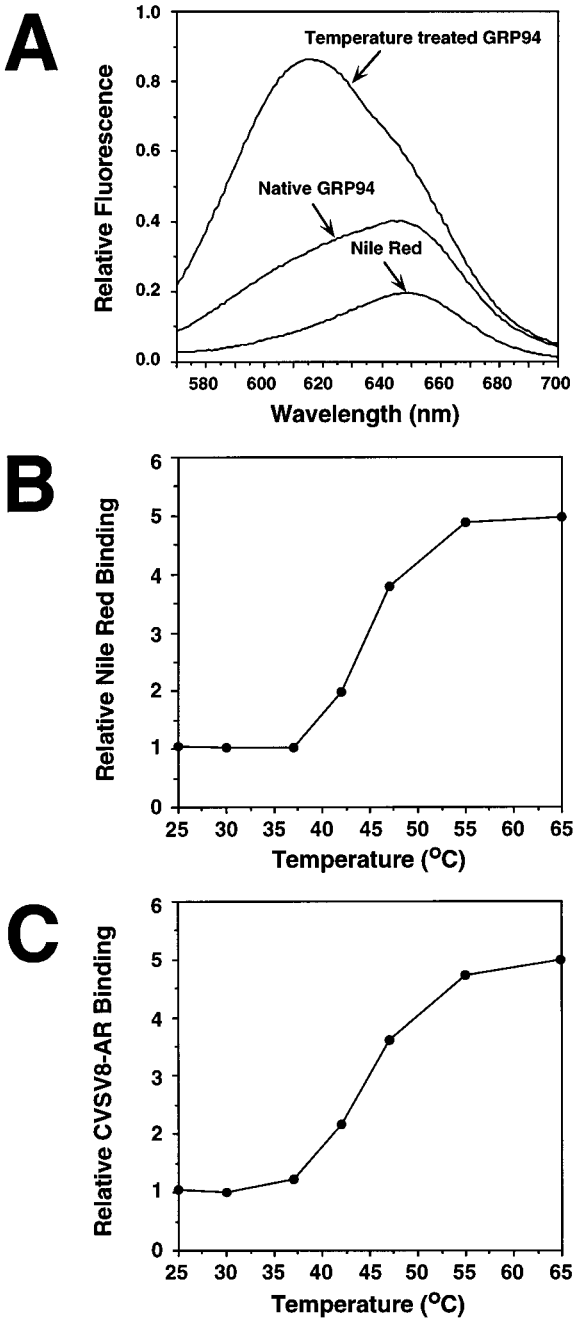

FIGURE 3: Binding of the environment-sensitive fluorophore Nile Red to GRP94: Comparison with peptide binding. (A) Native and temperature-treated GRP94 were incubated at a concentration of 0.5 μM with 1 μM Nile Red for 15 min at 37 °C. The emission spectra were recorded from 570 to 700 nm with an excitation wavelength of 550 nm and slit widths of 1 nm. (B) Temperature dependence of Nile Red binding. GRP94 (0.5 μM) was incubated with Nile Red (1 μM) for 15 min at the temperatures indicated. The fluoresence intensity at 615 nm, with excitation at 550 nm, was used to determine Nile Red binding. The data are representative of two separate experiments. (C) Temperature dependence of peptide binding. GRP94 (1.0 μM) was incubated with 20 nM VSV8−AR for 30 min at the temperatures indicated. The fluoresence intensity at 460 nm, with excitation at 360 nm, was taken as a measure of the binding of VSV8−AR to GRP94. The data are representative of two separate experiments.

α-helical content was observed following exposure to 5 M GdmCl (data not shown and Figure 4A). When the GdmCl-denatured samples were renatured following dialysis, the recovery of secondary structure was always greater than 90% (Figure 4A). The far-UV CD spectra of native and temper-

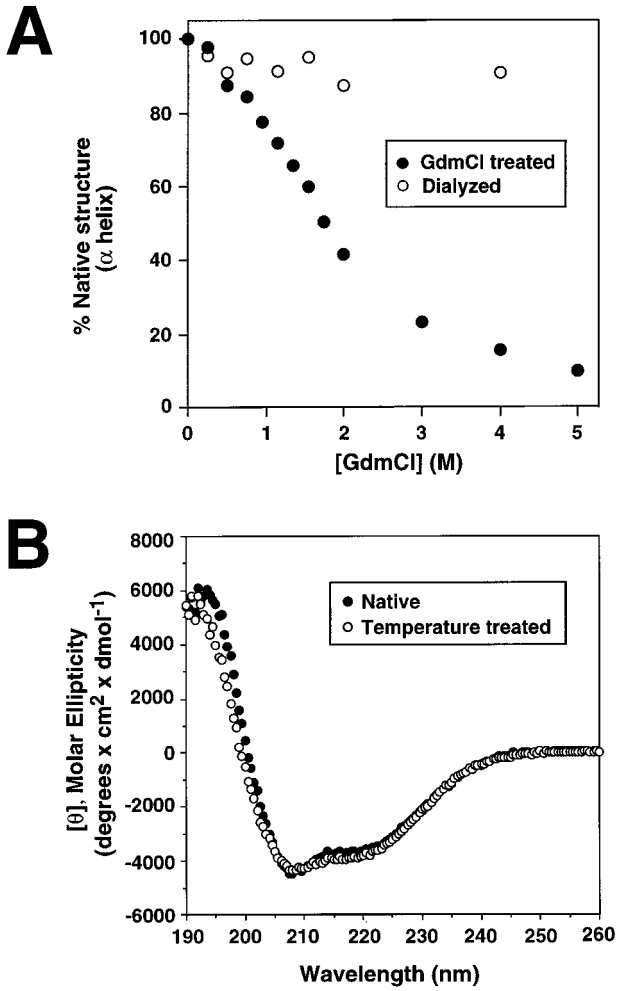

FIGURE 4: Far-UV CD analysis of the secondary structure of GRP94 after temperature and GdmCl treatments. (A) Denaturation and renaturation of GRP94 in GdmCl. The molar ellipticity at 222 nm was monitored as a measure of the α-helical content of GRP94 at increasing concentrations of GdmCl (●). Samples were then dialyzed to remove the denaturant and reanalyzed to determine the refolding efficiency (○). The percent native structure is expressed relative to the control sample of GRP94 with no GdmCl added. (B) The far-UV CD spectra for 1.25 μM native and temperature-treated GRP94 were analyzed at RT in 50 mM KOAc, 10 mM K-Hepes, pH 7.2. The mean residue ellipticity was calculated using a mean residue molecular weight of 118. Native (●); temperature-treated (○).

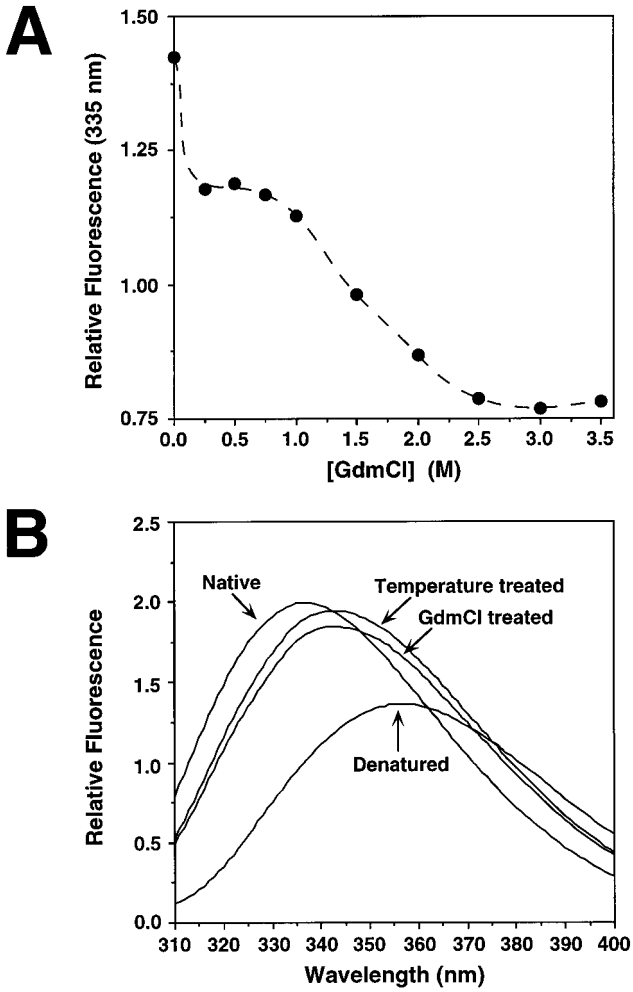

FIGURE 5: Detection of changes in GRP94 tertiary structure by tryptophan fluorescence. (A) The changes in the intrinsic fluorescence of GRP94 (75 μg/mL) were monitored in increasing concentrations of GdmCl. Excitation was set at 295 nm to exclusively monitor changes in the tryptophan fluorescence, and emission was monitored at 335 nm. The data are representative of two separate experiments. (B) The tryptophan emission spectra for native, GdmCl-treated, temperature-treated, and denatured GRP94 were determined. The GRP94 concentration was set at 75 μg/mL. GRP94 was denatured by addition of 3 M GdmCl which is present in the sample during analysis.

ature-treated GRP94 are shown in Figure 4B and were essentially identical. These data indicate that GRP94 displays a very high degree of native secondary structure following chemical denaturation/renaturation or transient heat shock.

Tertiary Structural Changes Accompany the Activation of Peptide Binding to GRP94. Analysis of GRP94 secondary structure for the native, GdmCl-treated, and temperature-treated forms of GRP94 indicated that the activation of peptide binding was not accompanied by significant changes in protein secondary structure. To determine whether changes in tertiary structure accompanied denaturation/renaturation or transient heat shock, tryptophan fluorescence and proteolysis studies were performed. When the changes in tryptophan fluorescence were monitored upon unfolding of GRP94 in increasing concentrations of GdmCl, a biphasic curve was observed (Figure 5A). At low GdmCl concentrations (<0.25 M), a decrease in fluorescence occurred; no further changes were observed at GdmCl concentrations up to 1 M (Figure 5A). Note that under identical conditions, no significant decrease in secondary structure could be discerned by far-UV CD (Figure 4A), suggesting that at low GdmCl concentrations GRP94 undergoes a limited tertiary structural change. The temperature dependence of the GRP94 tryptophan fluorescence was also determined and indicated a structural transition near 50 °C (data not shown).

To determine whether the observed tertiary structural transitions, as identified through tryptophan fluorescence, were reversible, the tryptophan emission spectra of native, temperature-treated, and GdmCl-treated GRP94 were determined (Figure 5B). Following excitation at 295 nm, the tryptophan fluorescence of native GRP94 displayed an emission maximum of 335 nm. A red-shift in the emission maxima to 343 nm and slight decrease in fluorescence were observed for GdmCl-treated and temperature-treated GRP94 (Figure 5B). When compared to the spectrum of GRP94 denatured in 3 M GdmCl (Figure 5B), these changes are

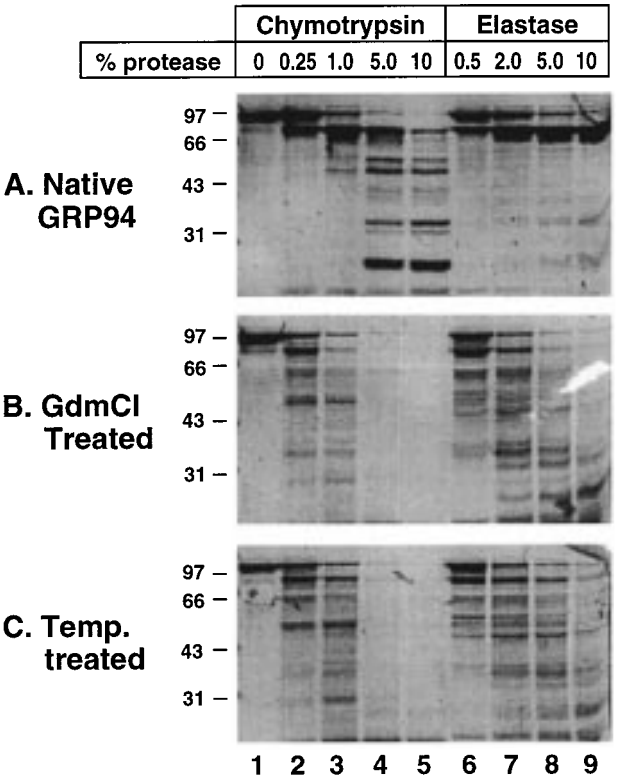

FIGURE 6: Protease digestion patterns provide evidence for a conformational change upon temperature and GdmCl treatments. Native (A), GdmCl-treated (B), or temperature-treated GRP94 (C) were incubated at a concentration of 0.15 mg/mL with the indicated concentrations (w/w) of chymotrypsin or elastase for 20 min at 30 °C. The digestion reaction was stopped by the addition of 10% TCA, and samples were analyzed by 10% SDS−PAGE.

significant, but relatively small. Such spectral changes are commonly observed upon increased solvent exposure of tryptophan side chains, and are indicative of tertiary structure differences (*47*). It is important to note that the structural differences appear to be irreversible and thus appear to represent at least two discrete structural states of the protein.

The conformational changes occurring upon temperature and GdmCl treatments were also investigated by protease mapping. In these experiments, native, temperature-treated, and GdmCl-treated GRP94 were incubated with increasing concentrations of chymotrypsin or elastase for 20 min at 30 °C. Limited digestion of native GRP94 with either enzyme generated a stable fragment of approximately 80 kDa (Figure 6A, lanes 2−3, 7−9) that has been previously identified as an N-terminal domain (*42*). The protease patterns for temperature-treated and GdmCl-treated GRP94 were notably different from native GRP94, but strikingly similar to one another. As with native GRP94, the N-terminal 80 kDa fragment was generated at low concentrations of chymotrypsin or elastase for both activated forms of the protein. However, this fragment displayed enhanced sensitivity to digestion at higher protease concentrations (Figure 6B,C, lanes 3, 7, and 8) and was markedly degraded at the 5−10% weight fraction of chymotrypsin (Figure 6B, lanes 4 and 5). These data, in context of the results depicted in Figure 5, are consistent with the interpretation that a tertiary conformational change accompanies the activation of GRP94 peptide binding activity.

Temperature-Induced Formation of Higher Order Oligomers Is Independent of the Increase in Peptide Binding Activity. Members of the Hsp90 molecular chaperone family share a high degree of sequence homology and in the native state are dimeric (*42*, *48*−*51*). It has previously been reported that heat shock promotes the formation of higher molecular weight oligomers of Hsp90, and, coincident with such changes in protein quaternary structure, a stimulation of chaperone activity (*52*). To investigate the effect of temperature and GdmCl treatments on GRP94 quaternary structure, native and activated GRP94 were analyzed by gel filtration chromatography. Native GRP94 eluted with a Stokes radius (R_s) of 7.4 nm (Figure 7A). In contrast, the elution volumes of GdmCl-treated and temperature-treated GRP94 were somewhat broader and significantly smaller, indicating an increase in the oligomeric state of the protein. The approximate molecular weights for these species were calculated from the R_s and sedimentation coefficient (data not shown) and indicated that a fraction of GRP94 molecules remained as dimers, while the shifted peaks represented tetramers and, to a lesser extent, higher order oligomers. This conclusion was confirmed by analytical ultracentrifugation (data not shown).

The formation of tetramers and higher order oligomers following temperature treatment was found to be highly dependent on GRP94 concentration. Thus, incubation of GRP94 at 50 °C at low concentrations did not significantly alter the average elution volume relative to native GRP94, whereas incubation at higher concentrations produced oligomers which eluted beyond the linear calibration range of the column (Figure 7B). To determine if the temperature-dependent increase in GRP94 oligomerization state was responsible for the activation of peptide binding activity, GRP94 was preincubated at 50 °C for 15 min at concentrations ranging from 0.5 to 15 μM, and peptide binding activity was assayed at a concentration of 0.5 μM GRP94. As shown in Figure 7B, a small, statistically insignificant increase in the peptide binding activity was observed with increasing oligomeric state, indicating that the formation of higher order oligomers is not responsible for the increase in peptide binding activity. Similar results were obtained using the fluorescence-based peptide binding assay (data not shown).

Peptide Binding to Activated GRP94 Is Independent of ATP and ADP. Recent crystal structure studies of the N-terminal domain of Hsp90 (*33*) identify low-affinity ATP/ADP binding to the binding pocket structurally identical to the geldanamycin binding site reported by Stebbins et al. (*34*). Although previous studies have indicated that peptide binding to native GRP94 is independent of ATP (*39*), the hypothesis that a regulatory role for ATP or ADP in peptide binding to GRP94 would be apparent in the activated protein was evaluated. As the reported dissociation constants for ATP and ADP binding to the Hsp90 N-terminal domain are high (132 and 29 μM, respectively) (*33*), equilibrium ATP binding studies were performed with 100 μM [α-^{32}P]ATP and a rapid, vacuum filtration method. A 50-fold excess of unlabeled ATP or ADP was included in the binding reactions to determine the binding specificity. As a positive control, ATP binding to BiP, a known ATPase, was analyzed in parallel (*53*). As shown in Figure 8A, 0.77 pmol of ATP was bound per picomole of BiP, and binding was inhibited by 95% and 46% by excess ATP and ADP, respectively. Similar to previous reports (*39*), very low, but detectable levels of ATP binding were observed for native GRP94 (0.08

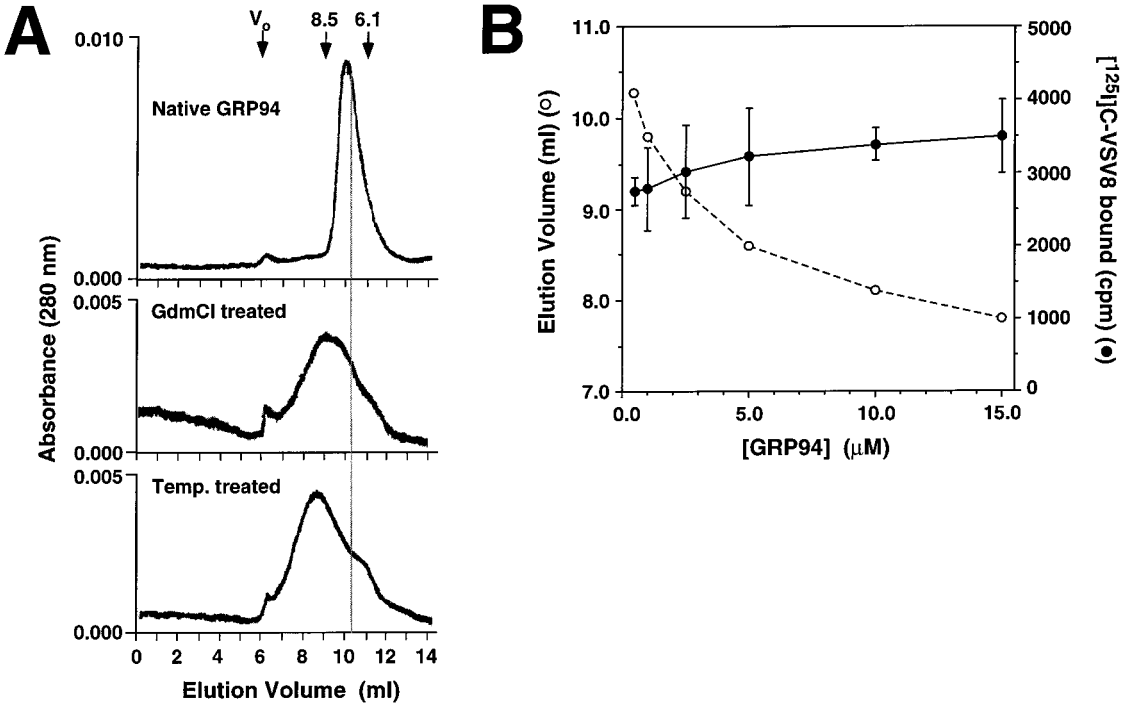

FIGURE 7: Analysis of GRP94 quaternary structure following temperature and GdmCl treatments. (A) The elution profiles for 25 μg of native, GdmCl-treated, and temperature-treated GRP94 were determined by analytical gel filtration chromatography. V_o = void volume. The numbers and arrows above the profiles indicate the elution volume and R_s for known molecular mass standards: thyroglobulin, 8.5 nm, 660 kDa; apoferritin, 6.1 nm, 440 kDa. (B) Concentration dependence of the formation of higher order GRP94 oligomers. GRP94 at concentrations from 0.5 to 15 μM was heated at 50 °C for 15 min, and the average elution volume was determined by analytical gel filtration. To determine the relationship between the oligomerization state and peptide binding activity, GRP94 was temperature-pretreated at concentrations ranging from 0.5 to 15 μM, adjusted to 0.5 μM, and incubated with 10 μM [^{125}I] C-VSV8 for 90 min at 37 °C. The amount of [^{125}I]C-VSV8 bound to GRP94 (●) was determined by gel filtration chromatography and plotted in parallel with the elution volume (○). For comparison, native, untreated GRP94 eluted at 10.4 mL and bound 840 cpm of [^{125}I]C-VSV8.

pmol of ATP/pmol of GRP94); however, even lower levels of ATP binding (0.03 pmol of ATP/pmol of GRP94) were observed for temperature-treated GRP94 (Figure 8A). It is important to note that BSA displayed similar low levels of ATP binding, which, as observed for GRP94, could be reduced with excess ATP or ADP (see legend to Figure 8).

The effects of ATP and ADP on peptide binding were also assayed under pseudo-first-order reaction conditions using the VSV8−AR binding assay. For these experiments, 1 μM temperature-treated GRP94 was incubated with 20 nM VSV8−AR in the absence or presence of 100 μM ATP or ADP. The emission spectra revealed that there were no differences in the amount of VSV8−AR bound in the presence of ATP or ADP (Figure 8B). Furthermore, there was also no change in the kinetics of VSV8−AR association with native or activated GRP94 in the presence of adenine nucleotides (data not shown).

DISCUSSION

Investigations into the immunological basis by which vaccination with GRP94 elicits CD8$^+$ T cell responses to GRP94−host cell antigens, as well as recent studies of the peptide binding activity of lumenal ER proteins, have unequivocally identified GRP94 as a peptide binding protein (*14*, *28*, *29*, *31*, *39*). Coincident with these observations, both in vivo and in vitro studies have indicated that GRP94 binds a diverse array of peptides, a subset of which display structural features appropriate for assembly onto nascent MHC class I molecules (*14*, *28*, *29*, *31*, *39*). That the transfer of GRP94-associated peptides onto MHC class I molecules can occur following immunization of mice with GRP94−peptide complexes identifies a significant functional characteristic of the GRP94−peptide binding reaction. That is, purified GRP94−peptide complexes are kinetically stable, yet, upon internalization into professional antigen presenting cells, peptide release and exchange onto class I molecules occurs, thereby yielding cell surface expression of class I molecules in association with GRP94-derived peptides. These observations imply that peptide binding to GRP94 is a regulated process, and that accelerated peptide exchange may occur in a cell- and/or compartment-specific manner. This conclusion is further supported by observations that peptide dissociation from isolated GRP94−peptide complexes is extremely slow (data not shown).

To gain insight into the regulation of GRP94 peptide binding activity, we have initiated studies into the structural basis of the peptide binding reaction. In the studies described herein, a number of structural correlates to the peptide binding reaction have been identified. Foremost, two conditions have been identified which yield a stable activation of specific peptide binding: transient heat shock and a cycle of chemical denaturation/renaturation. Analysis of protein secondary structure by far-UV circular dichroism spectroscopy indicated that the activated state was not accompanied by discernible alterations in GRP94 α-helical content. Rather, activation was associated with differences in protein tertiary structure, as displayed through GRP94 tryptophan fluorescence and mild proteolysis. Of particular interest, the activation of peptide binding directly correlated with the appearance of a hydrophobic pocket(s). Comparisons of the

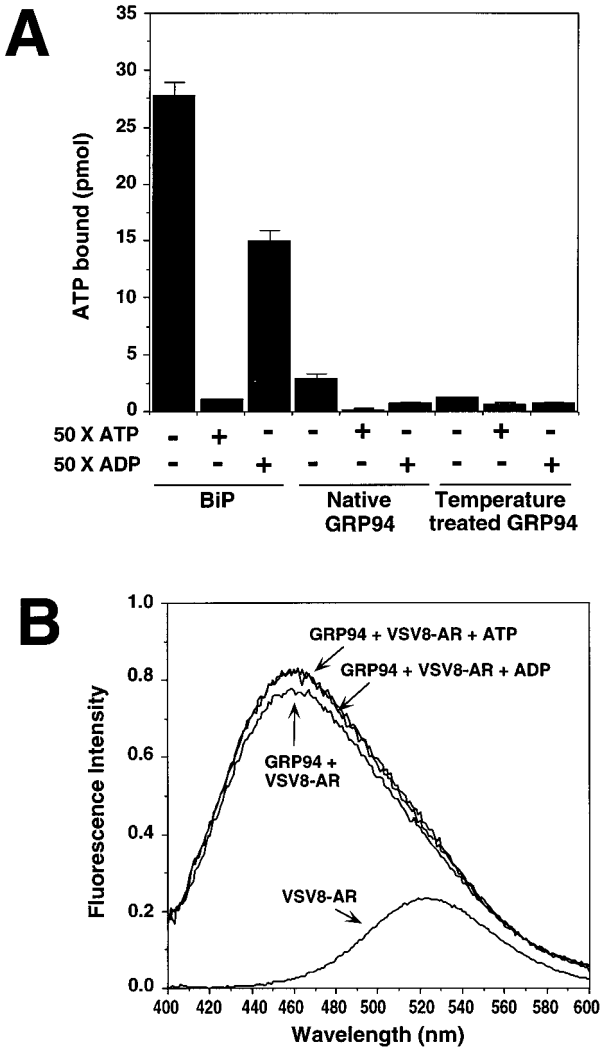

FIGURE 8: Binding of peptide to native and activated GRP94 is independent of adenine nucleotides. (A) The ATP binding properties of native and activated GRP94 were evaluated in parallel with BiP and BSA. Protein samples at 0.35 μM were incubated with 100 μM [α-^{32}P]ATP for 30 min at RT in the absence or presence of 5 mM ATP or ADP. The bound nucleotide was separated from free by vacuum filtration on nitrocellulose filters. Reactions were performed in triplicate. For comparison, BSA bound 1.85 pmol of [α-^{32}P]ATP in the absence of excess adenine nucleotides, 0.27 pmol in the presence of excess ATP, and 0.53 pmol in the presence of excess ADP. (B) Effect of adenine nucleotides on the binding of peptides to activated GRP94. Temperature-treated GRP94 (1 μM) was incubated with 20 nM VSV8−AR in the absence or presence of 100 μM ATP or ADP for 30 min at 37 °C. The emission spectra were recorded from 400 to 600 nm with an excitation wavelength of 360 nm.

emission spectra of the probes used to identify the pocket-(s) (Nile Red and acrylodan) indicated that the physical properties of the binding sites in the temperature-treated and GdmCl-treated GRP94 were identical, or reflected the appearance of more than one binding domain of very similar physical characteristics. In this regard, it should also be noted that the binding pocket was identified in binding studies of a peptide reporter conjugate as well as through direct solvent access of an environment-sensitive probe.

The data reported in this study are consistent with a two-stage model for peptide binding to GRP94. In this model, GRP94 can exist in either of two conformations, "open" or "closed". Native GRP94 would preferentially exist in the "closed" conformation and would be unable to bind peptide, or would bind slowly, whereas in the "open" conformation peptide binding is accelerated. Conversion from the "closed" to the "open" conformation would require a conformational change that can be mimicked, in vitro, by either transient heat shock or chemical denaturation/renaturation. With regard to heat shock, it is likely that conversion from the "closed" to the "open" conformation reflects a direct, thermally activated conformational change. The appearance of activated peptide binding following chemical denaturation/renaturation may reflect a differential recovery of two similar, but obviously distinct, structural states. Whether recovery of the "open" conformation upon renaturation is driven by simple stochastic processes or reflects a preferred conformation remains to be determined. In studying the purified protein in vitro, the majority of the native protein appears to reside in the "closed" conformation, and, on the basis of the tumor immunology and related studies, likely contains bound peptide. This assumption is currently under investigation. In this state, the transition to the active or "open" conformation occurs infrequently, thereby accounting for the kinetic stability of the GRP94−peptide complexes. We postulate that interconversion between the two forms is subject to regulation, possibly through physical interaction with other resident ER proteins, and/or through covalent modification. It is noteworthy that the structural behavior of GRP94, with respect to peptide binding, closely mirrors that proposed by Stebbins et al. (*34*) regarding the Hsp90 N-terminal domain. That is, this domain can be identified in two forms, "open" and "closed", and in the "closed" form accessibility to a hydrophobic pocket is blocked by a loop structure (L2) which serves an apparent gating function.

The described characteristics of the GRP94−peptide binding reaction, in particular the slow binding of peptide and the correlations between a stable structural transition and the activation of peptide binding, bear distinct similarities to another peptide binding protein, MHC class II. In studies of peptide binding to insect cell-expressed HLA-DR1 molecules, Sagdeh-Nasseri et al. (*54*) observed that kinetically stable peptide binding to soluble HLA-DR1 molecules required a structural transition that was only infrequently encountered, thereby yielding remarkably slow peptide binding. In the absence of such a structural transition, peptide binding occurred rapidly, but was accompanied by equally rapid dissociation, and did not yield a stable DR1−peptide complex (*54*). In a manner also similar to GRP94, peptide binding to MHC class II molecules requires the enhanced solvent exposure of a hydrophobic pocket (*55*, *56*). That the loading of peptide binding into MHC class II molecules is aided by the chaperone-like activity of DM-A and DM-B (*57*−*59*) suggests, by analogy, that there may exist proteins in the ER that perform an analogous function for GRP94. Thus, the kinetics of peptide binding to peptide binding proteins can be quite complex and often reflect both a conformation-driven binding site accessibility component and the rather extensive network of binding interactions that occur between the residues of the binding site and the different peptide atoms (*60*−*62*).

Crystal structure studies of the highly conserved N-terminal structural domain of Hsp90 have yielded potentially significant insights into the regulation of Hsp90−substrate interactions. Structure studies of the yeast Hsp90 N-terminal

domain indicate the presence of a domain-swapped dimer, with a potential peptide binding pocket residing within the central domain interface region (*33*). Furthermore, the N-terminal domain has been cocrystallized with bound ADP and ATP in the conserved binding pocket identified by Stebbins et al. (*34*) as the geldanamycin binding site, and postulated by these authors to also serve as a potential peptide binding pocket. In direct functional assays, we have been unable to identify a role for ADP or ATP in the regulation of peptide binding to GRP94, nor have we been able to identify substantial ATP binding activity (Figure 8; *39*). In addition, in preliminary experiments, we have observed no binding of GRP94 to geldanamycin beads coupled through the R3 position, although binding of Hsp90 was observed, and no substantial effects of geldanamycin on peptide binding to GRP94 (P. A. Wearsch, and C. V. Nicchitta, unpublished observations). The precise mechanistic basis for these apparent differences between the behavior of GRP94 and cytosolic Hsp90 is under investigation.

On a related note, it deserves mention that studies into the oligomeric structure of Hsp90 and GRP94 indicate that the C-terminal dimerization domain assembles the two subunits in an antiparallel configuration that maintains the N-termini in structural apposition (*42*, *51*). In view of these data, it would appear unlikely that an N-terminal dimer-interface is a structural feature of the native molecule. Firm conclusions regarding the site(s) of peptide binding must, however, await direct mapping studies and structural studies of stable peptide/domain complexes. It should also be mentioned that although the geldanamycin binding pocket has been proposed to serve as a potential site of peptide binding, recent studies of VSV8 binding to cytosolic Hsp90 identify the C-terminal assembly domain, for which detailed structure is not yet available, as the peptide VSV8 binding site (*63*).

ACKNOWLEDGMENT

We are grateful to Dr. Jim Wassenberg for valuable comments on the manuscript, to Dr. Vann Bennett (HHMI, Duke University Medical Center) for providing generous access to the CD spectrometer, to Dr. Steve Cala (Wayne State University, Detroit, MI) for polyclonal antisera to the N-terminus of GRP94, and to Dr. Len Neckers (NCI) for a generous supply of geldanamycin and geldanamycin beads.

REFERENCES

1. Shiu, R. P. C., Pouyssegur, J., and Pastan, I. (1977) *Proc. Natl. Acad. Sci. U.S.A. 74*, 3840−3844.
2. Welch, W. J., Garrels, J. I., Thomas, G. P., Lin, J. J.-C., and Feramisco, J. R. (1983) *J. Biol. Chem. 258*, 7102−7111.
3. Whelan, S. A., and Hightower, L. E. (1985) *J. Cell Physiol. 1995*, 251−258.
4. Kozutsumi, Y., Segal, M., Normington, K., Gething, M.-J., and Sambrook, J. (1988) *Nature 332*, 462−464.
5. Lenny, N., and Green, M. (1991) *J. Biol. Chem. 266*, 20532−20537.
6. Schaiff, W. T., Hruska, K. A., Jr., McCourt, D. W., Green, M., and Schwartz, B. D. (1992) *J. Exp. Med. 176*, 657−666.
7. Ferreira, L., Norris, K., Smith, T., Hebert, C., and Sauk, J. J. (1994) *J. Cell. Biochem. 56*, 518−526.
8. Melnick, J., Dul, J. L., and Argon, Y. (1994) *Nature (London) 370*, 373−375.
9. Kuznetsov, G., Chen, L. B., and Nigam, S. K. (1994) *J. Biol. Chem. 269*, 22990−22995.
10. Srivastava, P. K., DeLeo, A. B., and Old, L. J. (1986) *Proc. Natl. Acad. Sci. U.S.A. 83*, 3407−3411.
11. Udono, H., and Srivastava, P. K. (1994) *J. Immunol. 152*, 5398−5403.
12. Srivastava, P. K., Chen, Y. T., and Old, L. J. (1987) *Proc. Natl. Acad. Sci. U.S.A. 84*, 3807−3811.
13. Arnold, D., Faath, S., Rammensee, H.-G., and Schild, H. (1995) *J. Exp. Med. 182*, 885−889.
14. Suto, R., and Srivastava, P. K. (1995) *Science 269*, 1585−1588.
15. Nieland, T. J. F., Tan, M. C. A. A., Muijen, M. M.-V., Koning, F., Kruisbeek, A. M., and Van Bleek, G. M. (1996) *Proc. Natl. Acad. Sci. U.S.A. 93*, 6135−6139.
16. Tamura, Y., Peng, P., Liu, K., Daou, M., and Srivstava, P. K. (1997) *Science 278*, 117−120.
17. Udono, H., Levey, D. L., and Srivastava, P. K. (1994) *Proc. Natl. Acad. Sci. U.S.A. 91*, 3077−3081.
18. Germain, R. N. (1994) *Cell 76*, 287−299.
19. Nicchitta, C. V. (1998) *Curr. Opin. Immunol. 10*, 103−109.
20. Ortmann, B., Androwlewicz, M. J., and Cresswell, P. (1994) *Nature (London) 368*, 864−867.
21. Suh, W.-K., Cohen-Doyle, M. F., Fruh, K., Wang, K., Petersen, P. A., and Williams, D. B. (1994) *Science 264*, 1322−1326.
22. Sadasivan, B., Lehner, P. J., Ortman, B., Spies, T., and Cresswell, P. (1996) *Immunity 5*, 103−114.
23. Ortman, B., Copeman, J., Lehner, P. J., Sadasivan, B., Herberg, J. A., Grandea, A. G., Riddell, S. R., Tampe, R., Spies, T., Trowsdale, J., and Cresswell, P. (1997) *Science 277*, 1306−1309.
24. Anderson, K., Cresswell, P., Gammon, M., Hermes, J., Williamson, A., and Zweerink, H. (1991) *J. Exp. Med. 174*, 489−492.
25. Wei, M. L., and Cresswell, P. (1992) *Nature (London) 356*, 443−446.
26. Greenwood, R., Shimizu, Y., Sekhon, G. S., and Demars, R. (1994) *J. Immunol. 153*, 5525−5536.
27. Levy, F., Gabathuler, R., Larsson, R., and Kvist, S. (1991) *Cell 67*, 265−274.
28. Arnold, D., Wahl, C., Faath, S., Rammensee, H.-G., and Schild, H. (1997) *J. Exp. Med. 186*, 461−466.
29. Lammert, E., Arnold, D., Nijenhuis, M., Momburg, F., Häamerling, G. J., Brunner, J., Stevanovic, S., Rammensee, H.-G., and Schild, H. (1997) *Eur. J. Immunol. 27*, 923−927.
30. Marusina, K., Reid, G., Gabathuler, R., Jefferies, W., and Monaco, J. J. (1997) *Biochemistry 36*, 856−863.
31. Spee, P., and Neefjes, J. (1997) *Eur. J. Immunol. 27*, 2441−2449.
32. Gupta, R. S. (1995) *Mol. Biol. Evol. 12*, 1063−1073.
33. Prodromou, C., Roe, S. M., O'Brien, R., Ladbury, J. E., Piper, P., and Pearl, L. (1997) *Cell 90*, 65−75.
34. Stebbins, C. E., Russo, A. A., Schneider, C., Rosen, N., Hartl, F. U., and Pavletich, N. P. (1997) *Cell 89*, 239−250.
35. Bohen, S. P., and Yamamoto, K. R. (1993) *Proc. Natl. Acad. Sci. U.S.A. 90*, 11424−11428.
36. Sullivan, W. P., and Toft, D. O. (1993) *J. Biol. Chem. 268*, 20373−20379.
37. Kimura, Y., Matsumoto, S., and Yahara, I. (1994) *Mol. Gen. Genet. 242*, 517−527.
38. Nathan, D. F., and Lindquist, S. (1995) *Mol. Cell. Biol. 15*, 3917−3925.
39. Wearsch, P. A., and Nicchitta, C. V. (1997) *J. Biol. Chem. 272*, 5152−5156.
40. Prendergast, F. G., Meyer, M., Carlson, G. L., Iida, S., and Potter, J. D. (1983) *J. Biol. Chem. 258*, 7541−7544.
41. Chen, Y. H., Yang, J. T., and Chau, K. H. (1974) *Biochemistry 13*, 3350−3359.
42. Wearsch, P. A., and Nicchitta, C. V. (1996) *Biochemistry 35*, 16760−16769.
43. Blachere, N. E., Li, Z., Chandawarkar, R. Y., Suto, R., Jaikaria, N. S., Basu, S., Udono, H., and Srivsatava, P. K. (1997) *J. Exp. Med. 186*, 1315−1322.
44. Schmid, D., Baici, A., Gehring, H., and Christen, P. (1994) *Science 263*, 971−973.

45. Fekkes, P., den Blaauwen, T., and Driessen, A. J. M. (1995) *Biochemistry 34*, 10078−10085.
46. Sackett, D. L., and Wolff, J. (1987) *Anal. Biochem. 167*, 228−234.
47. Kassenbrock, C. K., and Kelly, R. B. (1989) *EMBO J. 8*, 1461−1467.
48. Koyasu, S., Nishida, E., Kadowaki, T., Matsuzaki, F., Iida, K., Harada, F., Kasuga, M., Sakai, H., and Yahara, I. (1986) *Proc. Natl. Acad. Sci. U.S.A. 83*, 8054−8058.
49. Iannotti, A. M., Rabideau, D. A., and Dougherty, J. J. (1988) *Arch. Biochem. Biophys. 264*, 54−60.
50. Minami, Y., Kawasaki, H., Miyata, Y., Suzuki, K., and Yahara, I. (1991) *J. Biol. Chem. 266*, 10099−10103.
51. Nemoto, T., Ohara-Nemoto, Y., Ota, M., Takagi, T., and Yokoyama, K. (1995) *Eur. J. Biochem. 233*, 1−8.
52. Yonehara, M., Minami, Y., Kawata, Y., Nagai, J., and Yahara, I. (1996) *J. Biol. Chem. 271*, 2641−2645.
53. Schmid, F. X. (1990) Spectral methods of characterizing protein conformation and conformational changes. In *Protein Structure: A Practical Approach* (Creighton, T. E., Ed.) IRL Press, New York.
54. Sadegh-Nasseri, S., Stern, L. J., Wiley, D. C., and Germain, R. N. (1994) *Nature (London) 370*, 647−650.
55. Boniface, J. J., Lyons, D. S., Wettstein, D. A., Albritton, N. L., and Davis, M. M. (1996) *J. Exp. Med. 183*, 119−126.
56. Runnels, H. A., Moore, J. C., and Jensen, P. E. (1996) *J. Exp. Med. 183*, 127−136.
57. Denzin, L. K., and Cresswell, P. (1995) *Cell 82*, 155−165.
58. Sherman, M. A., Weber, D. A., and Jensen, P. E. (1995) *Immunity 3*, 197−205.
59. Sloan, V. S., Cameron, P., Porter, G., Gammon, M., Amaya, M., Mellins, E., and Zaller, D. M. (1995) *Nature (London) 375*, 802−806.
60. Freemont, D. H., Matsumara, M., Stura, E. A., Peterson, P. A., and Wilson, I. A. (1992) *Science 257*, 919−927.
61. Silver, M. L., Guo, H. C., Strominger, J. L., and Wiley, D. C. (1992) *Nature (London) 360*, 367−369.
62. Stern, L. J., Brown, J. H., Jardetzky, T. S., Gorga, J. C., Urban, R. G., Strominger, J. L., Wiley, D. C. (1994) *Nature (London) 368*, 215−221.
63. Young, J. C., Schneider, C., and Hartl, F. U. (1997) *FEBS Lett. 418*, 139−143.

BI9801006